

Influence of the impurity scattering on charge transport in unconventional superconductor junctions

Bo Lu¹, Pablo Burset¹, Yasunari Tanuma², Alexander A. Golubov^{3,6}, Yasuhiro Asano^{4,5,6}, Yukio Tanaka^{1,6}

¹ *Department of Applied Physics, Nagoya University, Nagoya 464-8603, Japan*

² *Graduate School of Engineering Science, Akita University, Akita 010-8502, Japan*

³ *Faculty of Science and Technology and MESA+ Institute for Nanotechnology, University of Twente, 7500 AE Enschede, The Netherlands*

⁴ *Department of Applied Physics, Hokkaido University, Sapporo 060-8628, Japan*

⁵ *Center of Topological Science and Technology, Hokkaido University, Sapporo 060-8628, Japan*

⁶ *Moscow Institute of Physics and Technology, Dolgoprudny, Moscow 141700, Russia*

(Dated: April 22, 2016)

We study the influence of non-magnetic impurity scatterings on the tunneling conductance of a junction consisting of a normal metal and a disordered unconventional superconductor by solving the quasiclassical Eilenberger equation self-consistently. We find that the impurity scatterings in both the Born and unitary limits affect the formation of the Andreev bound states and modify strongly the tunneling spectra around zero bias. Our results are interpreted well by the appearance of odd-frequency Cooper pairs near the interface and by the divergent behavior of the impurity self-energy. The present paper provides a useful tool to identify the pairing symmetry of unconventional superconductors in experiments.

PACS numbers: 74.45.+c, 74.50.+r, 74.20.Rp

I. INTRODUCTION

The effects of impurity scatterings on superconducting phenomena are a key issue in the field of superconductivity. While the BCS s-wave pairing state is robust against nonmagnetic impurities¹, unconventional pairing states with other symmetries are usually rather fragile^{2–6}. The impurity scatterings modify transport and thermodynamic properties of unconventional superconductors, which has a crucial impact on the identification of the pairing symmetry, e.g., in *p*-wave superconductors^{7–9}. Specifically, the tunneling spectroscopy is an important experimental tool to identify an unconventional superconductor. The formation of the Andreev bound states at the surface of a superconductor is attributed to the anisotropy in the pairing states^{7,10–12} displaying a pronounced zero-bias conductance peak (ZBCP) in the tunneling conductance. In some cases, such bound states have a topological origin due to the bulk-edge correspondence^{13–21}. Therefore, the ZBCP in the tunneling conductance strongly suggests unconventional pairing symmetries of a superconductor.

Theoretically, the tunneling spectroscopy is formulated as a differential conductance in a normal metal/superconductor junction. Although effects of the potential disorder on the conductance have been studied in a number of papers, many of them focus on the disorder in the normal metal^{22–25}. Surprisingly, only few attempts have been made at the effects of disorder in the superconductor. Exceptional examples may be the studies about the proximity effect²⁶ and the ZBCP in high-T_c cuprate junctions. It is found that the broadened ZBCP can be explained by the impurity scatterings in the superconductor or the surface roughness^{27–30}. Although *p*-wave or chiral *p*-wave superconductors are a recent topic

of interest, effects of disorder in such superconductors have not yet been systematically studied. For instance, we have never known if the dome-like subgap conductance in chiral *p*-wave superconductors^{31–33} is robust or not in the presence of impurities. Similarly, chiral *d*- and chiral *f*-wave symmetries have been recently suggested to explain the absence of spontaneous edge currents in Sr₂RuO₄^{34,35}, where the sensitivity of the chiral edge current to potential disorder depends on chiral pairing symmetries³⁶. Several theoretical papers propose that doped graphene at a van Hove singular point may develop a chiral *d*-wave pairing state^{37–40}, which may be sensitive to weak impurity potentials treated within the Born limit. Furthermore, there are increasing evidences that suggest the strong impurity potential in Sr₂RuO₄^{41–44}. Theoretically, such strong impurities scatterings should be described by the unitary limit^{45,46}. As a result, a plethora of novel systems require a detailed analysis of the impurity effects on unconventional pairings in both weak and strong impurity limits.

In this article, we present a self-consistent calculation of the tunneling spectra in a normal-metal/disordered-superconductor junction with flat or chiral surface band states. For the former case, occurring in nodal superconductors, we find that the symmetry of the emergent odd-frequency pairing states^{25,47–50} plays a pivotal role in determining the evolution of the ZBCP under the impurity scatterings. As for chiral superconductors, our results show that the influence of the impurity scattering on the zero bias conductance in the unitary limit is more pronounced than that in the Born limit. It is important to emphasize that the disorder strength we consider is still below the diffusive (or Usadel) limit⁵¹. In that case, the strong pair-breaking effect would make the unconventional superconductor gapless.

The remainder of this paper is organized as follows. In section II, we describe our model and derive the essential formulas. In section III, we discuss impurity effects in junctions with nodal superconductors. The order parameters and tunneling spectroscopy are studied. In section IV, we show our result for chiral superconductors. Some concluding remarks are given in section V.

II. MODEL AND FORMALISM

Let us consider a two-dimensional normal metal-superconductor junction with a flat interface at $x = 0$ as shown in Fig.1. The interface barrier potential is de-

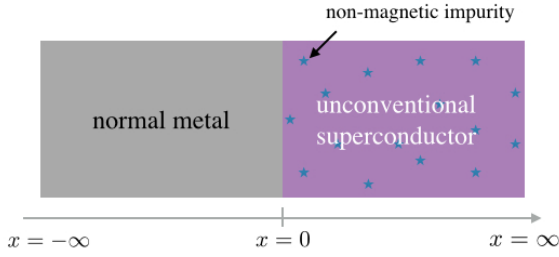


FIG. 1. (Color online) Schematic illustration of a normal metal/unconventional superconductor junction with a flat interface at $x = 0$. We assume impurities in superconducting side.

scribed by a delta function $V(x) = H\delta(x)$, with H the potential strength. The normal metal ($x < 0$) is assumed to be clean while the superconductor ($x > 0$) has a uniform impurity distribution. We denote the quasiclassical Green's function⁵²⁻⁵⁵ by $\hat{g}^{\alpha\alpha}(i\omega_n, x, \theta_\alpha)$, with Matsubara frequency $\omega_n = (2n+1)\pi T$, temperature T , and an integer n . θ_\pm is given by $\theta_+ \equiv \theta \in [-\pi/2, \pi/2]$ and $\theta_- = \pi - \theta$. We focus on the spin-degenerate system where $\hat{g}^{\alpha\alpha}(i\omega_n, x, \theta_\alpha)$ is a 2×2 matrix in particle-hole space satisfying Eilenberger equation⁵⁶

$$iv_f \cos \theta \partial_x \hat{g}^{\alpha\alpha} + \alpha \left[i\omega_n \hat{\tau}_3 - \hat{\Delta}(\theta_\alpha, x) \hat{\tau}_3 - \hat{a}(x), \hat{g}^{\alpha\alpha} \right] = 0, \quad (1)$$

accompanied by the normalization condition $(\hat{g}^{\alpha\alpha})^2 = -1$. Here v_f is the quasi-particle Fermi velocity and $\hat{\tau}_i$ are Pauli matrices. $\hat{\Delta}(\theta_\alpha, x)$ and $\hat{a}(x)$ are the superconducting order parameter and the self-energy induced by impurities, respectively. In the normal metal region, $\hat{\Delta}(\theta_\alpha, x < 0) = \hat{a}(x < 0) = 0$. We consider superconductors with different kinds of pairing symmetries: d_{xy} , p_x , p_y , and chiral states, so it is convenient to express the order parameter in the superconducting side $x > 0$ as

$$\hat{\Delta}(\theta_\alpha, x) = -\Delta_1(x, \theta_\alpha) \hat{\tau}_2 + \Delta_2(x, \theta_\alpha) \hat{\tau}_1. \quad (2)$$

For d_{xy} -, p_x -, and p_y - waves, $\Delta_1(x, \theta_\alpha) = 0$ and the gap equation $\Delta_2(x, \theta_\alpha) = \Delta(x) \chi(\theta_\alpha)$ is given by using the

quasi-classical Green's function as

$$\Delta(x) = \frac{2T \sum_{0 < \omega_m < \omega_c, \alpha} \int_{-\pi/2}^{\pi/2} d\theta' \chi(\theta'_\alpha) [\hat{g}^{\alpha\alpha}(i\omega_m, \theta'_\alpha, x)]_{12}}{\ln \frac{T}{T_c} + \sum_{0 < m < \frac{\omega_c}{2\pi T}} \frac{1}{m - 1/2}},$$

where $\chi(\theta_\alpha)$ is chosen as $\cos \theta_\alpha$ (p_x -wave), $\sin \theta_\alpha$ (p_y -wave), and $\sin 2\theta_\alpha$ (d_{xy} -wave). T_c and ω_c are the critical temperature of the bulk superconductor and the Debye frequency, respectively. For chiral wave states, $\Delta_1(x, \theta_\alpha) = \Delta_{im}(x) \chi_{im}(\theta_\alpha)$ and $\Delta_2(x, \theta_\alpha) = \Delta_{re}(x) \chi_{re}(\theta_\alpha)$ are given by

$$\Delta_{re}(x) = \frac{\sum_{0 < \omega_m < \omega_c, \alpha} \int_{-\pi/2}^{\pi/2} d\theta' \chi_{re}(\theta'_\alpha) [\hat{g}^{\alpha\alpha}(i\omega_m, \theta'_\alpha, x)]_{12}}{\frac{1}{2T} \left(\ln \frac{T}{T_c} + \sum_{0 < m < \frac{\omega_c}{2\pi T}} \frac{1}{m - 1/2} \right)},$$

and

$$\Delta_{im}(x) = \frac{\sum_{0 < \omega_m < \omega_c, \alpha} \int_{-\pi/2}^{\pi/2} d\theta' \chi_{im}(\theta'_\alpha) [\hat{g}^{\alpha\alpha}(i\omega_m, \theta'_\alpha, x)]_{12}}{\frac{i}{2T} \left(\ln \frac{T}{T_c} + \sum_{0 < m < \frac{\omega_c}{2\pi T}} \frac{1}{m - 1/2} \right)},$$

with

$$\begin{aligned} \chi_{re}(\theta_\alpha) &= \cos(\lambda \theta_\alpha), \\ \chi_{im}(\theta_\alpha) &= \sin(\lambda \theta_\alpha). \end{aligned}$$

We only consider the cases with chiral p -wave ($\lambda = 1$), chiral d -wave ($\lambda = 2$), and chiral f -wave ($\lambda = 3$).

The self-energy in the superconducting side can be decomposed as $\hat{a} = a_1 \hat{\tau}_1 + a_2 \hat{\tau}_2 + a_3 \hat{\tau}_3$ and is connected to the quasiclassical Green's function by

$$a_j(i\omega_m, x) = -\frac{1}{2\tau} \frac{\frac{1}{1-\sigma} \sum_\alpha \langle g_j^{\alpha\alpha}(i\omega_m, x) \rangle_\theta}{1 - \frac{\sigma}{1-\sigma} \sum_{i,\alpha} \langle g_i^{\alpha\alpha}(i\omega_m, x) \rangle_\theta^2}, \quad (3)$$

with $\hat{g}^{\alpha\alpha} = \sum_i g_i^{\alpha\alpha} \hat{\tau}_i$. Here, $1/\tau$ and σ denote the normal scattering rate and strength of a simple impurity potential, respectively. In the Born limit one finds that $\sigma \rightarrow 0$, while in the unitary limit $\sigma \rightarrow 1$, resulting in

$$\hat{a} = \begin{cases} -\frac{1}{2\tau} \sum_\alpha \langle \hat{g}^{\alpha\alpha} \rangle & \text{(Born limit)} \\ \frac{1}{2\tau} \left[\sum_\alpha \langle \hat{g}^{\alpha\alpha} \rangle \right]^{-1} & \text{(unitary limit)} \end{cases} \quad (4)$$

In the superconducting region, the Riccati parameterization⁵⁷⁻⁵⁹ is

$$\hat{g}^{++} = \frac{i}{1 - \mathcal{G}_+^S \mathcal{F}_+^S} \begin{bmatrix} 1 + \mathcal{G}_+^S \mathcal{F}_+^S & 2i \mathcal{F}_+^S \\ 2i \mathcal{G}_+^S & -1 - \mathcal{G}_+^S \mathcal{F}_+^S \end{bmatrix}, \quad (5)$$

$$\hat{g}^{--} = \frac{i}{\mathcal{G}_-^S \mathcal{F}_-^S - 1} \begin{bmatrix} 1 + \mathcal{G}_-^S \mathcal{F}_-^S & 2i\mathcal{F}_-^S \\ 2i\mathcal{G}_-^S & -1 - \mathcal{G}_-^S \mathcal{F}_-^S \end{bmatrix}. \quad (6)$$

The Riccati parameters \mathcal{G}_\pm^S , \mathcal{F}_\pm^S obey the equations

$$v_f \cos \theta \partial_x \mathcal{G}_+^S = 2\tilde{\omega}_n \mathcal{G}_+^S - \Lambda_{2+} + \Lambda_{1+} (\mathcal{G}_+^S)^2, \quad (7a)$$

$$v_f \cos \theta \partial_x \mathcal{F}_+^S = -2\tilde{\omega}_n \mathcal{F}_+^S - \Lambda_{1+} + \Lambda_{2+} (\mathcal{F}_+^S)^2, \quad (7b)$$

$$v_f \cos \theta \partial_x \mathcal{G}_-^S = -2\tilde{\omega}_n \mathcal{G}_-^S + \Lambda_{2-} - \Lambda_{1-} (\mathcal{G}_-^S)^2, \quad (7c)$$

$$v_f \cos \theta \partial_x \mathcal{F}_-^S = 2\tilde{\omega}_n \mathcal{F}_-^S + \Lambda_{1-} - \Lambda_{2-} (\mathcal{F}_-^S)^2, \quad (7d)$$

with the definitions

$$\tilde{\omega}_n = \omega_n + ia_3,$$

$$\Lambda_{1\pm} = i\Delta_{1\pm} + \Delta_{2\pm} - a_1 + ia_2,$$

$$\Lambda_{2\pm} = -i\Delta_{1\pm} + \Delta_{2\pm} + a_1 + ia_2.$$

At the interface $x = 0$, we have the boundary conditions^{57,59-61}

$$\mathcal{F}_+^S(x=0) \rightarrow \begin{cases} \frac{R}{\mathcal{G}_+^S(x=0)}, & \omega_n > 0, \\ \frac{1}{R\mathcal{G}_-^S(x=0)}, & \omega_n < 0, \end{cases} \quad (8)$$

$$\mathcal{F}_-^S(x=0) \rightarrow \begin{cases} \frac{1}{R\mathcal{G}_+^S(x=0)}, & \omega_n > 0, \\ \frac{R}{\mathcal{G}_-^S(x=0)}, & \omega_n < 0, \end{cases} \quad (9)$$

with $R = Z^2 / [Z^2 + 4 \cos^2 \theta]$, $Z = 2mH/k_f$, m the electron mass, and k_f the Fermi momentum. In this work, we only consider the low transmitting case with fixed $Z = 5$. The local density of states (LDOS) ρ_S is given by

$$\rho_S(x) = \frac{1}{\pi} \text{Im} \sum_{\alpha} \int_{-\pi/2}^{\pi/2} d\theta' \hat{g}^{\alpha\alpha} (i\omega_m \rightarrow E + i\delta, \theta'_\alpha, x)_{11} \quad (10)$$

To obtain the conductance, we write down the wave functions in terms of the Riccati parameter $\bar{\mathcal{G}}_\pm^S = \mathcal{G}_\pm^S(E, \theta_\pm, x=0)$ at the interface, which are

$$\begin{cases} \text{N: } \begin{bmatrix} 1 \\ a \end{bmatrix} e^{ik_f \cos \theta x} + \begin{bmatrix} b \\ 0 \end{bmatrix} e^{-ik_f \cos \theta x} \\ \text{S: } c \begin{bmatrix} 1 \\ i\bar{\mathcal{G}}_+^S \end{bmatrix} e^{ik_f \cos \theta x} + d \begin{bmatrix} -i[\bar{\mathcal{G}}_-^S]^{-1} \\ 1 \end{bmatrix} e^{-ik_f \cos \theta x} \end{cases},$$

with a, b (c, d) reflection (transmission) amplitudes. Using BTK theory⁶², we obtain the normalized differential conductance

$$\sigma_t = \int_{-\pi/2}^{\pi/2} d\theta \cos \theta \sigma_\theta / \sigma_n,$$

where $\sigma_\theta = 1 - |b|^2 + |a|^2$ reads^{12,63}

$$\sigma_\theta = \sigma_N \frac{|\bar{\mathcal{G}}_-^S|^2 + \sigma_N |\bar{\mathcal{G}}_+^S \bar{\mathcal{G}}_-^S|^2 + (\sigma_N - 1) |\bar{\mathcal{G}}_+^S|^2}{|\bar{\mathcal{G}}_-^S + (\sigma_N - 1) \bar{\mathcal{G}}_+^S|^2}, \quad (11)$$

with $\sigma_N = 4 \cos^2 \theta / [Z^2 + 4 \cos^2 \theta]$ and $\sigma_n = \int_{-\pi/2}^{\pi/2} d\theta \cos \theta \sigma_N$ the conductance in normal states. In the numerical calculations, we take the temperature $T = 0.05T_c$. For convenience, we do not consider thermodynamic phenomena and assume the Debye frequency $\omega_c = 2\pi$ for all the considered pairing states.

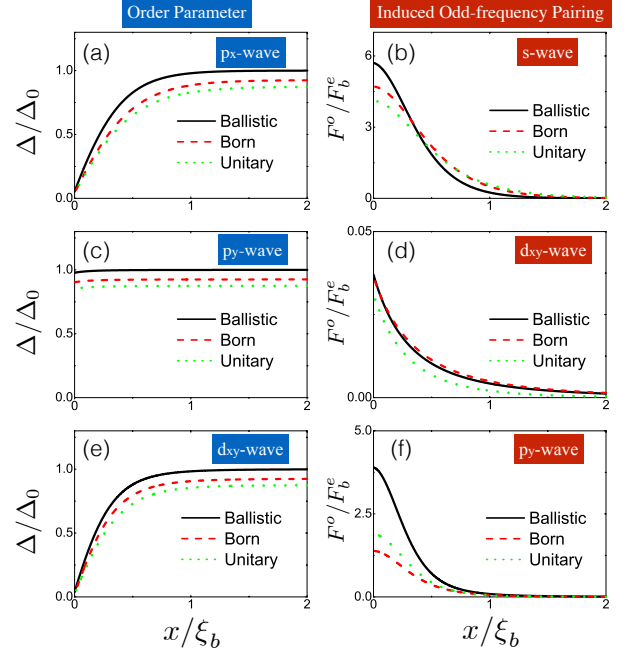


FIG. 2. (Color online) Order parameter amplitude (left) and induced odd-frequency pairing amplitude (right) near the interface between a superconductor and a normal metal. From top to bottom, (a)(b) p_x -wave, (c)(d) p_y -wave, and (e)(f) d_{xy} -wave.

III. NODAL SUPERCONDUCTORS WITH FLAT SURFACE BANDS

A. Order parameter and odd-frequency

First, we show the spacial variation of the order parameter amplitude in the left panels of Fig.2. Three regimes are considered: ballistic, Born, and unitary limit. In the ballistic case, the relaxation time becomes infinite so we set $1/\tau = 0$. For Born and unitary limit, it is given by $1/\tau = 0.2\Delta_b$, where Δ_b is the bulk value of the order parameter (in ballistic case, the value of the order parameter Δ_b is denoted by Δ_0). We define the superconducting coherence length as $\xi_b = v_f/\Delta_b$. We can see that for p_x - and d_{xy} -wave cases, the order parameters with or without impurities strongly decrease when they approach the interface. However, for the p_y case, the order parameter is almost invariant in space. For the following discussion of conductance spectra in this subsection, we plot the odd-frequency pairing states in the right panels of

Fig.2. The anomalous Green's function $\bar{F} = \sum_{\alpha} [\hat{g}^{\alpha\alpha}]_{12}$ can be decomposed into an even-frequency component $\bar{F}^e(i\omega_n, \theta) = \bar{F}^e(-i\omega_n, \theta)$ and an odd-frequency one $\bar{F}^o(i\omega_n, \theta) = -\bar{F}^o(-i\omega_n, \theta)$. The Fourier transform of $\bar{F}^{o(e)}$ is given by^{64–66}

$$\bar{F}^{o(e)}(i\omega_n, \theta) = \sum_m f_{c,m}^{o(e)} \cos(m\theta) + f_{s,m}^{o(e)} \sin(m\theta). \quad (12)$$

We denote by F^o the dominant odd-frequency component $f_{c,m}^o$ or $f_{s,m}^o$ and normalize it by the bulk value of the even-frequency component $F_b^e = f_{c,m}^e$ (with $m = 1, 2$ for p_x -, d_{xy} -wave, respectively) or $F_b^e = f_{s,1}^e$ (p_y -wave). It can be seen from the results that as the order parameter decreases in p_x - and d_{xy} -wave cases, a large value of odd-frequency component is generated near the interface which determines the shape of Cooper pairs to be s - and p_y -wave, respectively⁶⁴. One can compare the magnitudes of odd-frequency components in the presence of impurities with the ballistic case to find that the generated s -wave odd-frequency magnitude is not sensitive to the impurity scattering which is consistent with the Anderson theorem¹. In the d_{xy} -wave case, the non- s -wave odd frequency component is strongly suppressed as the impurity scattering is introduced. For p_y -wave case, the odd-frequency component is very small while the dominant pairing near the surface is even-frequency.

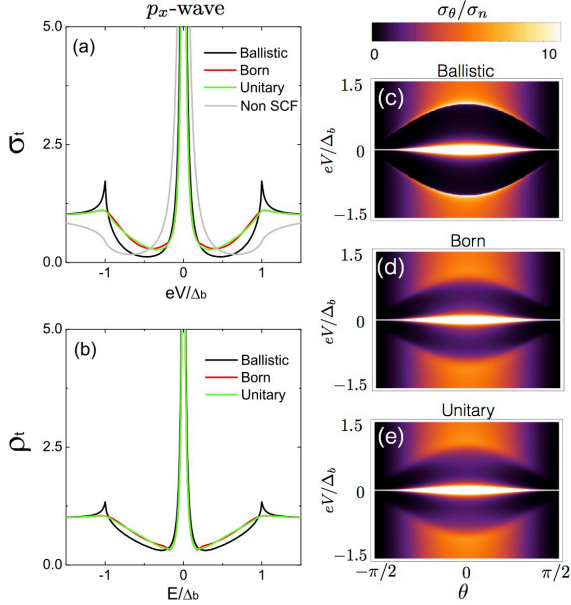


FIG. 3. (Color online) P_x -wave: (a) conductance and (b) local density of states at the normal metal-superconductor interface. Angle-resolved conductance for (c) ballistic, (d) Born, and (e) unitary limit.

B. Tunneling spectroscopy

We plot the normalized conductance σ_t for spin-triplet p_x -wave in Fig.3. For comparison, we also show the non-

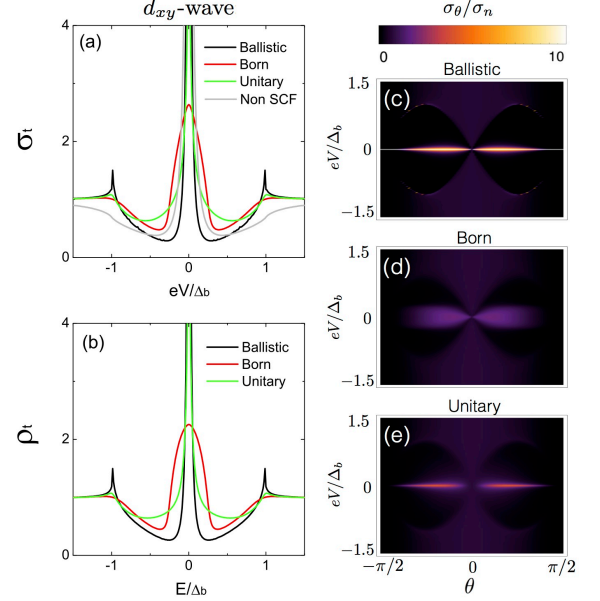


FIG. 4. (Color online) D_{xy} -wave: (a) conductance and (b) local density of states at the normal metal-superconductor interface. Angle-resolved conductance for (c) ballistic, (d) Born, and (e) unitary limit.

self-consistent (non-SCF) result (light gray line) and the LDOS $\rho_t = \rho_S / \rho_n$ at the interface $x = 0$, with ρ_n the density of states in the non-superconducting state. Although the p_x -wave superconductor has not been found in actual materials, it is becoming a topic of interest as a prototype for topological superconductivity^{13–21} and an increasing effort is dedicated to designing p_x -wave superconductors using materials with strong spin-orbit coupling^{67–71}. Our numerical calculation verifies the results of Ref. 71 about the robustness of the sharp ZBCP against impurities. Furthermore, we find that not only the height of ZBCP is robust but also the width does not broaden. For $eV \approx \Delta_b$, the ballistic case shows a sharp coherence peak which is smeared away in the presence of impurities. This is due to the energy level broadening by impurity effect as concluded from the angle-resolved conductance spectra σ_θ / σ_n plotted in Figs.3(d)(e). For comparison, we reproduce the conductance result of Ref. 29 for d_{xy} -wave superconductors in Fig.4. Although in the ballistic limit both p_x - and d_{xy} -wave superconductors show a sharp ZBCP, their conductance spectra under impurity scattering are quite different. The ZBCP for d_{xy} -wave broadens and is suppressed by impurities, specially in the Born limit. Figs. 4(d)(e) show a smeared low energy conductance in the angle-resolved conductance spectra compared to the ballistic case of Fig. 4(c). The impact of impurities on the ZBCP is shown in Fig. 5 for p_x - (black squares) and d_{xy} -wave (red triangles). Figs. 5(a)(b) show the evolution of the ZBCP as a function of the impurity scattering rate in the Born and unitary limits, respectively. The ZBCP for p_x -wave pairing is unaffected by changes in the scattering rate or the impurity strength,

shown in Fig. 5(c). On the other hand, the ZBCP for d_{xy} -wave pairing is very vulnerable to the presence of impurities, becoming rapidly suppressed. Next, we show the results for p_y -wave junctions in Fig. 6. In this case, the Andreev bound state is absent, resulting in a sharp zero bias conductance dip in the ballistic limit. For a fixed impurity density level, we find that the dip structure is more pronounced in the Born limit while it is greatly enhanced and smeared in the unitary limit.

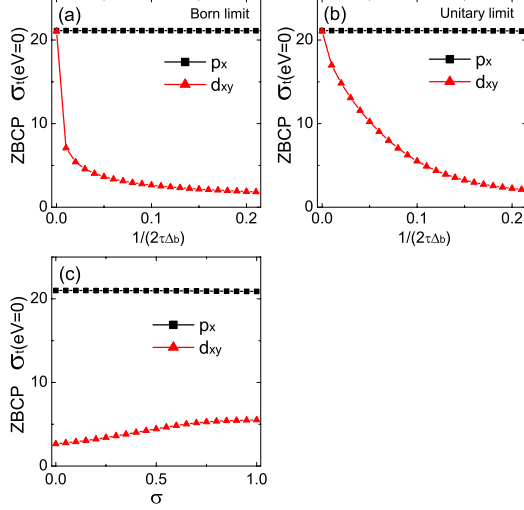


FIG. 5. (Color online) Zero bias conductance peak vs. impurity scattering. (a) In the Born limit, the ZBCP as a function of the density of impurities and (b) the same plot in the unitary limit. (c) Fixing $1/(2\tau\Delta_b)$ at 0.1, the ZBCP as a function of the impurity strength σ .

These three typical behaviors of zero bias conductance in nodal superconductors can be well interpreted from the symmetry of odd-frequency pairings and the divergent behavior of the self-energy. In the bulk, the Green's function $\hat{G}(E, \theta) = \sum_{\alpha} \hat{g}^{\alpha\alpha}(E, \theta_{\alpha})$ is only divergent when the energy locates at continuum levels. However, in the junction system, the spacial dependent Green's function $\hat{G}(E, x, \theta)$ can also develop a divergence near the surface (or interface) $x = 0$ due to the emergent Andreev bound state at $E = E_b$, $\theta = \theta_b$. For surface flat bands forming at angles connecting gap nodes, according to Eq. 4, the magnitude of the components a_i of the self-energy $\hat{a}(E = 0, x = 0)$ in the Born limit is expected to surpass that of their counterparts in the unitary limit for the same scattering rate $1/\tau$. Consequently, the ZBCP should be more sensitive to impurities in the Born limit than in the unitary limit, explaining the behavior of the d_{xy} -wave case. Further, we can also consider the symmetry of Cooper pairs near the interface. As previously discussed in Fig. 2, Cooper pairs at the interface of p_x -wave and d_{xy} -wave junctions are odd in frequency. For p_x -wave, Fermi-Dirac statistics impose that Cooper pairs form a spin-triplet isotropic s -wave state, making the pairings, together with the ZBCP, insensitive to impurities. This is a consequence of the ZBCP for p_x -wave

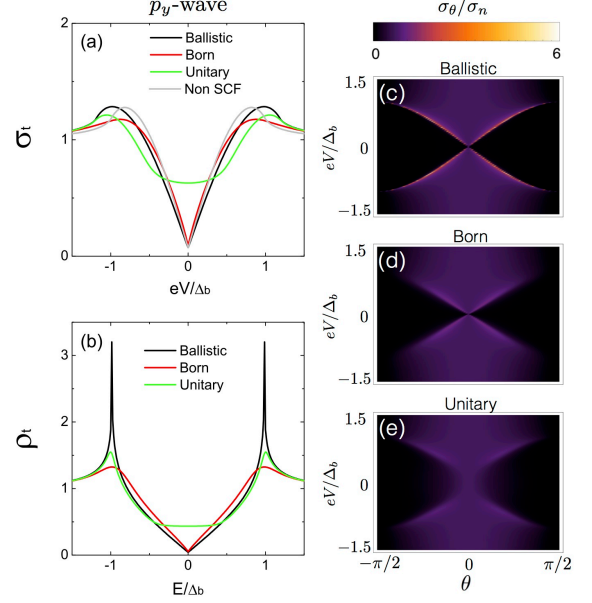


FIG. 6. (Color online) P_y -wave: (a) conductance and (b) local density of states at the normal metal-superconductor interface. Angle-resolved conductance for (c) ballistic, (d) Born, and (e) unitary limit.

junctions being protected by chiral symmetry⁷¹. For pairing symmetries like d_{xy} -wave, Cooper pairs form an odd-frequency spin-singlet p -wave pairing state which is dominant near the surface. Due to the anisotropy of the state, the ZBCP is more fragile. For pairing symmetries supporting no Andreev bound states, like the p_y -wave case, $\langle \hat{G}(E, x = 0, \theta) \rangle_{\theta}$ is approximately zero when the energy E is away from the continuum levels, which makes

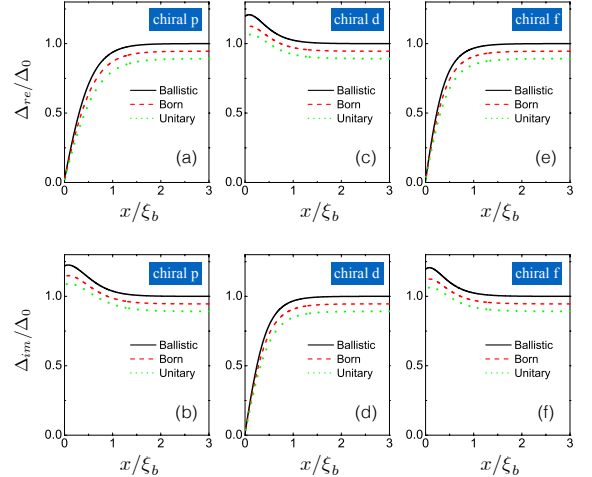


FIG. 7. (Color online) Spatial dependence of order parameters in chiral wave superconductors: (a)(b): chiral p -wave, (c)(d) chiral d -wave, and (e)(f) chiral f -wave. The upper panels show the real part of the order parameter and the lower ones the imaginary part.

the self-energy a_i more stronger in the unitary limit than in the Born limit. Thus, the conductance is more sensitive in the unitary limit as it is shown in Fig.6.

IV. GAPPFUL SUPERCONDUCTORS WITH CHIRAL SURFACE BANDS

In this section, we show the results of superconductors with chiral edge states. There is an increasing amount of evidence supporting that Sr_2RuO_4 is a candidate for a chiral p -wave superconductor^{41–44}. The gap parameter has the form $\mathbf{d} \propto (k_x + ik_y)^\lambda \hat{\mathbf{e}}_z$, where $\hat{\mathbf{e}}_z$ is a unit vector along the tetragonal crystal c -axis and $\lambda = 1$. However, such a chiral triplet superconductor features a spontaneous edge supercurrent which has not yet been observed in experiments. Several theories have suggested that λ could be larger than 1, e.g., $\lambda = 2$ (chiral d -wave) or $\lambda = 3$ (chiral f -wave), leading to a suppression of the edge current^{34,35}. Consequently, it is crucial to study the transport signatures of chiral d - or chiral f -wave states in Sr_2RuO_4 . The study of chiral d -wave superconducting states is also relevant since it has also been proposed in other systems, e.g., in doped-graphene^{37–40}.

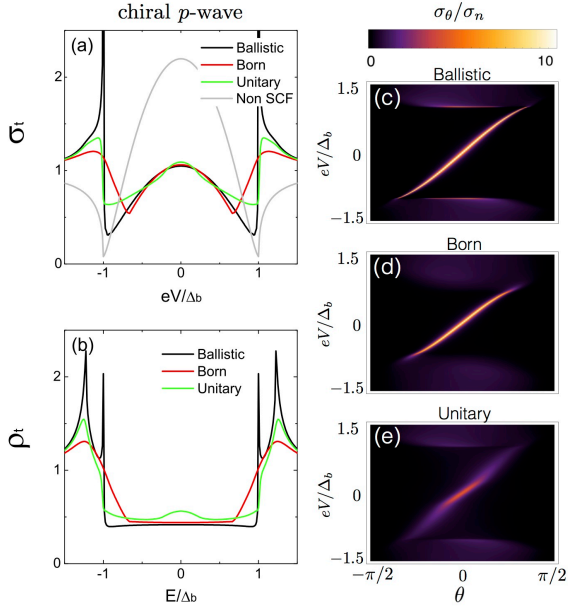


FIG. 8. (Color online) Chiral p -wave: (a) conductance and (b) local density of states at the normal metal-superconductor interface. Angle-resolved conductance for (c) ballistic, (d) Born, and (e) unitary limit.

First, we plot the spacial variance of order parameters in Fig.7. Chiral p -, d -, and f -waves display a similar behavior. The real and imaginary components of the order parameter vary in a different way as they approach the interface: one is slightly enhanced (real part for chiral d -wave and imaginary for chiral p - and f -wave), to a value denoted by Δ_{in} at the interface, and the other is greatly

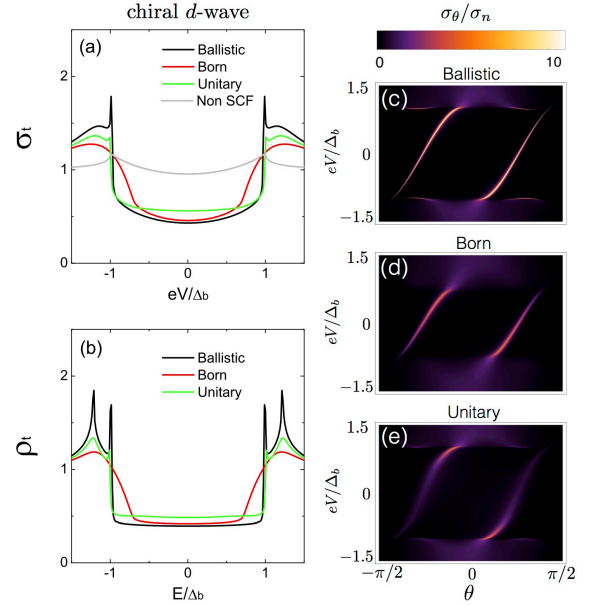


FIG. 9. (Color online) Chiral d -wave: (a) conductance and (b) local density of states at the normal metal-superconductor interface. Angle-resolved conductance for (c) ballistic, (d) Born, and (e) unitary limit.

suppressed. Such results have been revealed in previous studies of the BW phase of ^3He ^{7,72} or Sr_2RuO_4 ^{73–75}.

We now proceed to discuss the conductance and LDOS. In Fig.8, we show our results for chiral p -wave junctions. Compared to the non-SCF case (gray line), the dome-like ZBCP^{31–33} is still visible with or without impurity scattering, although reduced. Actually, the height of the ZBCP has a very weak dependence on the impurity potential. A conductance peak appears near the bulk gap $eV \approx \Delta_b$, especially sharp in the ballistic limit. Also in the ballistic case, there are double peaks in the LDOS located at the position of Δ_b and Δ_{in} [see Fig. 7(b)]⁷⁵. The subgap LDOS at the interface is finite and almost constant, just slightly convex, revealing the existing chiral Andreev bound state across the region $-\Delta_b < E < \Delta_b$. We note that although the value of the ZBCP and the subgap conductance qualitatively agrees with the experiments, the obtained SCF result does not reproduce the full tunneling spectra in Sr_2RuO_4 ^{76,77}. Thus, we consider that the self-consistent calculation in the framework of 3-bands model⁴³ in Sr_2RuO_4 is needed in the future.

Fig. 9 shows the LDOS and conductance spectroscopy for chiral d -wave superconductors. As can be seen from the LDOS in panel (b), the double peak structure outside the gap in the ballistic limit is prominent and still visible for the unitary case at $1/(2\tau\Delta_b) = 0.1$, while the peak at $E = \Delta_b$ is absent in the Born limit. For the conductance spectroscopy shown in panel (a), we emphasize the absence of ZBCP. The conductance features a wide concave bottom gap and its minimum is barely affected by the impurity scattering. Besides that, the double peak structure outside the gap is more visible in

the conductance spectroscopy in the ballistic and unitary limits. The angle-resolved conductance spectra in Fig. 9(c)(d)(e) display double chiral states owing to a Chern number $ch = 2^{78,79}$.

Finally, we show the results for chiral f -wave states in Fig. 10. The subgap conductance and LDOS are similar to chiral d -wave states as seen in panels (a) and (b). In the ballistic limit, the conductance peak at $eV \approx \Delta_b$ becomes small as compared to chiral p - and chiral d -wave case. The impurity effect does not change the bottom-like characteristic of conductance and LDOS inside the bulk gap. Here, the Chern number $ch = 3$ manifests three chiral Andreev bound states inside the gap as seen in Fig. 10(c)(d)(e). However, the slopes of the states are much higher than those of chiral p - and chiral d -wave pairings, reducing their contribution to the angle-averaged conductance. As a result, there are no ZBCP for the parameters we have used.

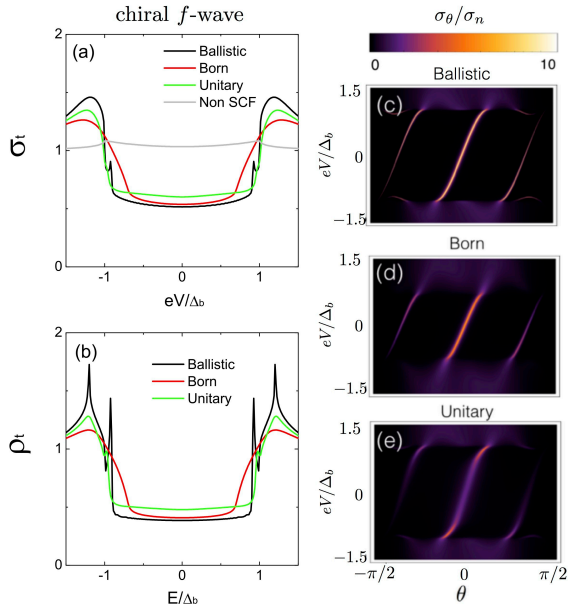


FIG. 10. (Color online) Chiral f -wave: (a) conductance and (b) local density of states at the normal metal-superconductor interface. Angle-resolved conductance for (c) ballistic, (d) Born, and (e) unitary limit.

Due to the characteristics of the tunneling spectroscopy and LDOS for chiral superconductors, it is convenient to discuss the impurity effect in three separated energy regions: (1) $E \sim 0$; (2) $E \sim \Delta_b$; (3) $E \sim \Delta_{in}$. Similarly to the previous section, let us focus on the divergence of the Green's function $\hat{G}(E, \theta)$. Compared to the flat surface bands, the density of zero energy states is greatly reduced leading to a finite but relatively small value of angle-averaged Green's function $\langle \hat{G}(E=0, x=0, \theta) \rangle_\theta$. Thus, for the same scattering rate $1/\tau$, the magnitude of the components a_i of the self-energy $\hat{a}(E=0, x=0)$ is more pronounced in the unitary limit than in the Born limit. Consequently, the zero

	ballistic [$\sigma_t(eV=0)$]	Born	unitary
p_x	peak ($\sigma_t \gg 1$)	\bigcirc	\bigcirc
p_y	dip ($\sigma_t = 0$)	\simeq	\sim
d_{xy}	peak ($\sigma_t \gg 1$)	--	-
chiral p	peak ($\sigma_t \sim 1$)	\simeq	\sim
chiral d	enhancement ($0 < \sigma_t < 1$)	\simeq	\sim
chiral f	enhancement ($0 < \sigma_t < 1$)	\simeq	\sim

TABLE I. Zero bias conductance vs. impurity scattering in the ballistic, Born and unitary limit. The label \bigcirc indicates the immunity to impurity scattering. \simeq (\sim) means the zero bias conductance is approximately similar (slightly increased). -- (--) means a decrease (strong decrease) of conductance with respect to the ballistic limit.

bias conductance and LDOS are more sensitive in the unitary limit. For $E \sim \Delta_b$ and $E \sim \Delta_{in}$, the appearance of continuum bands greatly enhances $\langle \hat{G}(E, x=0, \theta) \rangle_\theta$ and makes the self-energy terms a_i smaller. As a result, the unitary limit would retain the double peak structure mostly outside the bulk gap Δ_b (e.g., see panel (b) of Fig. 9). It is also easy to understand that the steep structure in the conductance and LDOS near $E \sim \Delta_b$ in the ballistic limit disappears easily in the Born limit. We have summarized the behavior of zero bias conductance in Table I.

V. CONCLUSION

In conclusion, we have theoretically studied the tunneling spectroscopy in normal metal-disordered unconventional superconductor junctions at low transparency for various pairing symmetries. For nodal superconductors with flat surface bands, the influence of the impurity scattering can be classified into three types according to the behavior of zero bias conductance: (1) when Cooper pairs at the surface have odd-frequency s -wave symmetry, the zero-bias conductance peak is immune to the impurity scattering; (2) for non s -wave odd-frequency pairing, the zero-bias conductance peak is strongly suppressed by impurities; and (3) in the accidental absence of Andreev bound states, the zero bias conductance dip is easily smeared by impurities in the unitary limit.

For chiral superconductors, we have shown the self-consistent result of conductance spectra and found that a zero-bias conductance peak for chiral p -wave pairings remains in the presence of impurities. The zero bias conductance for chiral waves is more sensitive to impurity scattering in the unitary limit than that in the Born limit. Moreover, the double peaks occurring in the LDOS and conductance spectra at the gap edges for all chiral waves are very sensitive to impurity scattering and are especially blurred in the Born limit. We expect that our results can be exploited for the experimental identification of pairing symmetries by analyzing the tunneling spectroscopy of unconventional superconductors.

ACKNOWLEDGMENTS

We thank M. Y. Kupriyanov, K. Yada, and S. V. Bakurskiy for valuable discussions. This work was supported by a Grant-in-Aid for Scientific Research on Innovative Areas Topological Material Science (Grant No. 15H05853), a Grant-in-Aid for Scientific Research B (Grant No. 15H03686), a Grant-in-Aid for Challenging Exploratory Research (Grant No. 15K13498) from

the Ministry of Education, Culture, Sports, Science, and Technology, Japan (MEXT); Japan-RFBR JSPS Bilateral Joint Research Projects/Seminars (Grants No. 15-52-50054 and No. 15668956); and Dutch FOM, the Ministry of Education and Science of the Russian Federation, Grant No. 14.Y26.31.0007 and by the Russian Science Foundation, Grant No. 15-12-30030. P.B. acknowledges support from JSPS International Research Fellowship.

-
- ¹ P. W. Anderson, *J. Phys. Chem. Solids* **11**, 26 (1959).
 - ² A. I. Larkin, *Zh. Eksp. Teor. Fiz.* **2**, 205 (1965), [*JETP Lett.* **2**, 130 (1965)].
 - ³ R. Balian and N. R. Werthamer, *Phys. Rev.* **131**, 1553 (1963).
 - ⁴ A. J. Millis, S. Sachdev, and C. M. Varma, *Phys. Rev. B* **37**, 4975 (1988).
 - ⁵ M. Sigrist and K. Ueda, *Rev. Mod. Phys.* **63**, 239 (1991).
 - ⁶ R. J. Radtke, K. Levin, H. B. Schuttler, and M. R. Norman, *Phys. Rev. B* **48**, 653 (1993).
 - ⁷ L. J. Buchholtz and G. Zwicknagl, *Phys. Rev. B* **23**, 5788 (1981).
 - ⁸ K. Maki and E. Puchkaryov, *Europhys. Lett.* **50**, 533 (2000).
 - ⁹ M. J. Graf and A. V. Balatsky, *Phys. Rev. B* **62**, 9697 (2000).
 - ¹⁰ C. Bruder, *Phys. Rev. B* **41**, 4017 (1990).
 - ¹¹ C. R. Hu, *Phys. Rev. Lett.* **72**, 1526 (1994).
 - ¹² S. Kashiwaya and Y. Tanaka, *Rep. Prog. Phys.* **63**, 1641 (2000).
 - ¹³ A. P. Schnyder, A. F. S. Ryu, and A. W. W. Ludwig, *Phys. Rev. B* **78**, 195125 (2008).
 - ¹⁴ M. Sato, *Phys. Rev. B* **79**, 214526 (2009).
 - ¹⁵ M. Sato, *Phys. Rev. B* **81**, 220504(R) (2010).
 - ¹⁶ M. Z. Hasan and C. L. Kane, *Rev. Mod. Phys.* **82**, 3045 (2010).
 - ¹⁷ S. Ryu, A. P. Schnyder, A. Furusaki, and A. W. W. Ludwig, *New J. Phys.* **12**, 065010 (2010).
 - ¹⁸ M. Z. Hasan and J. E. Moore, *Annu. Rev. Condens. Matter Phys.* **2**, 55 (2011).
 - ¹⁹ X. L. Qi and S. C. Zhang, *Rev. Mod. Phys.* **83**, 1057 (2011).
 - ²⁰ J. Alicea, *Rep. Prog. Phys.* **75**, 076501 (2012).
 - ²¹ Y. Tanaka, M. Sato, and N. Nagaosa, *J. Phys. Soc. Jpn.* **81**, 011013 (2012).
 - ²² Y. Tanaka, Y. V. Nazarov, and S. Kashiwaya, *Phys. Rev. Lett.* **90**, 167003 (2003).
 - ²³ Y. Tanaka and S. Kashiwaya, *Phys. Rev. B* **70**, 012507 (2004).
 - ²⁴ Y. Tanaka, S. Kashiwaya, and T. Yokoyama, *Phys. Rev. B* **71**, 094513 (2005).
 - ²⁵ Y. Tanaka and A. A. Golubov, *Phys. Rev. Lett.* **98**, 037003 (2007).
 - ²⁶ T. Löfwander, *Phys. Rev. B* **70**, 094518 (2004).
 - ²⁷ A. Poenicke, Y. S. Barash, C. Bruder, and V. Istyukov, *Phys. Rev. B* **59**, 7102 (1999).
 - ²⁸ A. A. Golubov and M. Y. Kupriyanov, *Pisma Zh. Eksp. Teor. Fiz.* **69**, 242 (1999), [*JETP Lett.* **69**, 262 (1999)].
 - ²⁹ Y. Tanaka, Y. Tanuma, and S. Kashiwaya, *Phys. Rev. B* **64**, 054510 (2001).
 - ³⁰ Y. Asano and Y. Tanaka, *Phys. Rev. B* **65**, 064522 (2002).
 - ³¹ M. Yamashiro, Y. Tanaka, and S. Kashiwaya, *Phys. Rev. B* **56**, 7847 (1997).
 - ³² C. Honerkamp and M. Sigrist, *Journal of Low Temperature Physics* **111**, 895 (1998).
 - ³³ M. Yamashiro, Y. Tanaka, Y. Tanuma, and S. Kashiwaya, *Journal of the Physical Society of Japan* **67**, 3224 (1998).
 - ³⁴ W. Huang, E. Taylor, and C. Kallin, *Phys. Rev. B* **90**, 224519 (2014).
 - ³⁵ Y. Tada, W. Nie, and M. Oshikawa, *Phys. Rev. Lett.* **114**, 195301 (2015).
 - ³⁶ S.-I. Suzuki and Y. Asano, arXiv:1602.03994 (2016).
 - ³⁷ A. M. Black-Schaffer and C. Honerkamp, *J. Phys.: Condens. Matter* **26**, 423201 (2014).
 - ³⁸ R. Nandkishore, L. S. Levitov, and A. V. Chubukov, *Nat. Phys.* **8**, 158 (2012).
 - ³⁹ W. S. Wang, Y. Y. Xiang, Q. H. Wang, F. Wang, F. Yang, and D. H. Lee, *Phys. Rev. B* **85**, 035414 (2012).
 - ⁴⁰ M. L. Kiesel, C. Platt, W. Hanke, D. A. Abanin, and R. Thomale, *Phys. Rev. B* **86**, 020507(R) (2012).
 - ⁴¹ Y. Maeno, H. Hashimoto, K. Yoshida, S. Nishizaki, T. Fujita, J. G. Bednorz, and F. Lichtenberg, *Nature* **372**, 532 (1994).
 - ⁴² C. Kallin, *Rep. Prog. Phys.* **75**, 042501 (2012).
 - ⁴³ A. P. Mackenzie and Y. Maeno, *Rev. Mod. Phys.* **75**, 657 (2003).
 - ⁴⁴ Y. Maeno, S. Kittaka, T. Nomura, S. Yonezawa, and K. Ishida, *J. Phys. Soc. Jpn.* **81**, 011009 (2012).
 - ⁴⁵ K. Miyake and O. Narikiyo, *Phys. Rev. Lett.* **83**, 1423 (1999).
 - ⁴⁶ M. Suzuki, M. A. Tanatar, N. Kikugawa, Z. Q. Mao, Y. Maeno, and T. Ishiguro, *Phys. Rev. Lett.* **88**, 227004 (2002).
 - ⁴⁷ V. L. Berezinskii, *JETP Letters* **20**, 287 (1974), [*Pisma Zh. Eksp. Teor. Fiz.* **20**, 628 (1974)].
 - ⁴⁸ T. R. Kirkpatrick and D. Belitz, *Phys. Rev. Lett.* **66**, 1533 (1991).
 - ⁴⁹ A. Balatsky and E. Abrahams, *Phys. Rev. B* **45**, 13125 (1992).
 - ⁵⁰ F. S. Bergeret, A. F. Volkov, and K. B. Efetov, *Rev. Mod. Phys.* **77**, 1321 (2005).
 - ⁵¹ K. D. Usadel, *Phys. Rev. Lett.* **25**, 507 (1970).
 - ⁵² J. W. Serene and D. Rainer, *Phys. Rep.* **101**, 221 (1983).
 - ⁵³ A. V. Zaitsev, *Zh. Eksp. Teor. Fiz.* **86**, 1742 (1984), [*Sov. Phys. JETP* **59**, 1015 (1984)].
 - ⁵⁴ A. Millis, D. Rainer, and J. A. Sauls, *Phys. Rev. B* **38**, 4504 (1988).
 - ⁵⁵ M. Ashida, S. Aoyama, J. Hara, and K. Nagai, *Phys. Rev. B* **40**, 8673 (1989).

- ⁵⁶ G. Eilenberger, Z. Phys. **214**, 195 (1968).
- ⁵⁷ Y. Nagato, K. Nagai, and J. Hara, J. Low Temp. Phys. **93**, 33 (1993).
- ⁵⁸ N. Schopohl and K. Maki, Phys. Rev. B **52**, 490 (1995).
- ⁵⁹ M. Eschrig, Phys. Rev. B **61**, 9061 (2000).
- ⁶⁰ M. Fogelström, Phys. Rev. B **62**, 11812 (2000).
- ⁶¹ E. Zhao, T. Löfwander, and J. A. Sauls, Phys. Rev. B **70**, 134510 (2004).
- ⁶² G. E. Blonder, M. Tinkham, and T. M. Klapwijk, Phys. Rev. B **25**, 4515 (1982).
- ⁶³ Y. Tanaka and S. Kashiwaya, Phys. Rev. Lett. **74**, 3451 (1995).
- ⁶⁴ Y. Tanaka, A. A. Golubov, S. Kashiwaya, and M. Ueda, Phys. Rev. Lett. **99**, 037005 (2007).
- ⁶⁵ M. Eschrig, T. Löfwander, T. Champel, J. C. Cuevas, J. Kopu, and G. Schön, Journal of Low Temperature Physics **147**, 457 (2007).
- ⁶⁶ Y. Tanaka, Y. Tanuma, and A. A. Golubov, Phys. Rev. B **76**, 054522 (2007).
- ⁶⁷ J. D. Sau, R. M. Lutchyn, S. Tewari, and S. D. Sarma, Phys. Rev. Lett. **104**, 040502 (2010).
- ⁶⁸ R. M. Lutchyn, J. D. Sau, and S. D. Sarma, Phys. Rev. Lett. **105**, 077001 (2010).
- ⁶⁹ Y. Oreg, G. Refael, and F. von Oppen, Phys. Rev. Lett. **105**, 177002 (2010).
- ⁷⁰ J. You, C. H. Oh, and V. Vedral, Phys. Rev. B **87**, 054501 (2013).
- ⁷¹ S. Ikegaya, Y. Asano, and Y. Tanaka, Phys. Rev. B **91**, 174511 (2015).
- ⁷² S. Higashitani, Y. Nagato, and K. Nagai, J. Low Temp. Phys. **155**, 83 (2009).
- ⁷³ M. Matsumoto and M. Sigrist, J. Phys. Soc. Jpn. **68**, 994 (1999).
- ⁷⁴ Y. Tanuma, Y. Tanaka, and S. Kashiwaya, Phys. Rev. B **74**, 024506 (2006).
- ⁷⁵ S. V. Bakurskiy, A. A. Golubov, M. Y. Kupriyanov, K. Yada, and Y. Tanaka, Phys. Rev. B **90**, 064513 (2014).
- ⁷⁶ F. Laube, G. Goll, H. v. Löhneysen, M. Fogelström, and F. Lichtenberg, Phys. Rev. Lett. **84**, 1595 (2000).
- ⁷⁷ S. Kashiwaya, H. Kashiwaya, H. Kambara, T. Furuta, H. Yaguchi, Y. Tanaka, and Y. Maeno, Phys. Rev. Lett. **107**, 077003 (2011).
- ⁷⁸ G. E. Volovik, JETP Lett. **70**, 609 (1999).
- ⁷⁹ S. Kashiwaya, H. Kashiwaya, K. Saitoh, Y. Mawatari, and Y. Tanaka, Physica E **55**, 25 (2014).